Interaction between Cytochrome *caa*$_3$ and F_1F_0-ATP Synthase of Alkaliphilic *Bacillus pseudofirmus* OF4 Is Demonstrated by Saturation Transfer Electron Paramagnetic Resonance and Differential Scanning Calorimetry Assays†

Xiaoying Liu,‡ Xing Gong,‡ David B. Hicks,§ Terry A. Krulwich,§ Linda Yu,*,‡ and Chang-An Yu*,‡

Department of Biochemistry and Molecular Biology, Oklahoma State University, Stillwater, Oklahoma 74078, and Department of Pharmacology and Biological Chemistry, Mount Sinai School of Medicine, One Gustave L. Levy Place, New York, New York 10029

Received September 14, 2006; Revised Manuscript Received November 6, 2006

ABSTRACT: Interaction between the cytochrome *caa*$_3$ respiratory chain complex and F_1F_0-ATP synthase from extremely alkaliphilic *Bacillus pseudofirmus* OF4 has been hypothesized to be required for robust ATP synthesis by this alkaliphile under conditions of very low protonmotive force. Here, such an interaction was probed by differential scanning calorimetry (DSC) and by saturation transfer electron paramagnetic resonance (STEPR). When the two purified complexes were embedded in phospholipid vesicles individually [(*caa*$_3$)PL, (F_1F_0)PL)] or in combination [(*caa*$_3$ + F_1F_0)PL] and subjected to DSC analysis, they underwent exothermic thermodenaturation with transition temperatures at 69, 57, and 46/75 °C, respectively. The enthalpy change, ΔH (−8.8 kcal/mmol), of protein−phospholipid vesicles containing both cytochrome *caa*$_3$ and F_1F_0 was smaller than that (−12.4 kcal/mmol) of a mixture of protein−phospholipid vesicles formed from each individual electron transfer complex [(*caa*$_3$)PL + (F_1F_0)PL]. The rotational correlation time of spin-labeled *caa*$_3$ (65 μs) in STEPR studies increased significantly when the complex was mixed with F_1F_0 prior to being embedded in phospholipid vesicles (270 μs). When the complexes were reconstituted separately and then mixed together, or either mitochondrial cytochrome *bc*$_1$ or F_1F_0 was substituted for the alkaliphile F_1F_0, the correlation time was unchanged (65−70 μs). Varying the ratio of the two alkaliphile complexes in both the DSC and STEPR experiments indicated that the optimal stoichiometry is 1:1. These results demonstrate a physical interaction between the cytochrome *caa*$_3$ and F_1F_0-ATP synthase from *B. pseudofirmus* OF4 in a reconstituted system. They support the suggestion that such an interaction between these complexes may contribute to sequestered proton transfers during alkaliphile oxidative phosphorylation at high pH.

During oxidative phosphorylation (OXPHOS)[1] in mitochondria and most bacteria, energy from the exergonic oxidation−reduction reactions of the electron transport chain is conserved in an electrochemical gradient of protons across the membrane, alkaline and negative inside relative to outside. This Δp is used to energize ATP synthesis by the proton-coupled ATP synthase (*1*). Protons moving downhill through the integral membrane a- and c-subunits of the F_0 sector of the synthase lead to rotation of the c-subunit rotor and the associated γ-subunit, causing conformational changes in the catalytic F_1 sector that result in ATP synthesis (*2*, *3*). The nature and involvement of the Δp as the crucial intermediate form of energy in OXPHOS were a major contribution of Mitchell's chemiosmotic hypothesis (*1*). The chemiosmotic formulation further posited that the proton path from the proton-extruding respiratory chain complexes to the ATP synthase was through the bulk liquid phase outside the mitochondrion or bacterial cell. By contrast, Williams and others proposed that greater efficiency of energy coupling would be achieved by transfer of protons without full equilibration with the bulk phase (*4*−*7*). Williams considered the possibility of actual protein−protein interactions, perhaps facilitated by special adaptations of the proteins and participation of membrane phospholipids (*6*). Other proposals have involved proton trapping at the outside membrane surface that creates a delocalized surface Δp that is functionally larger than the bulk force and obviates the need for specific adaptations of participating respiratory chain elements or the ATP synthase (*6*, *8*, *9*). The expectation is that the drugs or genetic variations that effect OXPHOS will depend upon the specifics of the proton path, i.e., (i) involvement of membrane lipid and protein surfaces versus (ii) additional involvement of protein−protein interactions versus (iii) only a bulk energization pathway of protons. Therefore, further definition of the proton path is important.

† This work was supported in part by Grants GM30721 (to C.-A.Y.) and GM028454 (to T.A.K.) from the National Institutes of Health.

* Corresponding author. Phone: (405) 744-6612. Fax: (405) 744-6612. E-mail: cayuq@okstate.edu.

‡ Oklahoma State University.

§ Mount Sinai School of Medicine.

[1] Abbreviations: OXPHOS, oxidative phosphorylation; ΔGp, phosphorylation potential; Δp, electrochemical proton gradient across the membrane; $\Delta\Psi$, transmembrane electrical potential (negative in); *caa*$_3$, cytochrome *caa*$_3$; DSC, differential scanning calorimetry; EPR, electron paramagnetic resonance; FRAP, fluorescence recovery after photobleaching; MSL, maleimide spin label (4-maleimido-2,2,6,6-tetramethyl-1-piperidine-*N*-oxyl); STEPR, saturation transfer electron paramagnetic resonance.

10.1021/bi0619167 CCC: $37.00
Published on Web 01/02/2007

OXPHOS by alkaliphilic *Bacillus* species that carry out proton-coupled ATP synthesis at pH values ≥10.5 has been an important experimental system for assessing models of the proton path (*10*−*12*). As studied in extremely alkaliphilic *Bacillus pseudofirmus* OF4, two properties of alkaliphile OXPHOS suggest that, above pH 9.5, ATP synthesis requires the bulk transmembrane electrical potential, $\Delta\Psi$, but also requires specific adaptations of the synthase that support proton transfer from the respiratory chain to the synthase without full equilibration with the bulk (*13*−*15*). First, OXPHOS is more robust at pH 10.5 than at pH 7.5. The phosphorylation potential, ΔGp, that directly relates to the steady-state force supporting synthesis is about −530 mV at pH 10.5 and −435 mV at pH 7.5. However, the bulk Δp is about 3 times lower at the higher pH because of the large, chemiosmotically adverse ΔpH (∼2.3 pH units, acid in relative to out) that is sustained by the Na^+/H^+ antiporter-dependent pH homeostasis mechanism (*13*). The capacity for OXPHOS at pH 10.5 depends upon alkaliphile-specific sequence features of the F_0-ATP synthase. Mutation of two of these features to the *Bacillus* consensus sequence resulted in a fully functional enzyme that supported OXPHOS at pH 7.5 but not at pH 10.5 (*15*). Second, large artificially imposed diffusion potentials fail to energize ATP synthesis above pH 9.5, where nonfermentative growth and respiration-dependent OXPHOS are optimal (*13*). This property reflects a blockage of proton flux both to and from the bulk phase at pH ≥9.5 that protects against cytoplasmic alkalinization during sudden exposure to high pH. Two residues of the F_0-ATP synthase a-subunit have been shown to participate in this pH-dependent proton "gating", one of which is also required for ATP synthesis at high pH (*15*). These findings led us to propose that a kinetically sequestered proton path from the respiratory chain to the ATP synthase at high pH is supported by properties of the participating complexes as well as the membrane and may involve dynamic protein−protein interactions between the ATP synthase and one of the terminal oxidases of the respiratory chain, the proton-pumping caa_3 oxidase. The expression of this oxidase is upregulated by either high pH or low Δp resulting from protonophore treatment (*16*, *17*), and mutations that reduce cytochrome caa_3 activity also prevent nonfermentative growth at high pH (*18*). Moreover, alignments show that alkaliphile cytochrome caa_3 has alkaliphile-specific sequence features that might contribute to interactions with the ATP synthase (e.g., an alkaliphile-specific T79 of subunit I and an unusually acidic region in subunit II in the putative proton path through the oxidase). Before initiating a mutagenesis study of such sequence features of cytochrome caa_3, we sought evidence for the putative protein−protein interactions.

Using methods of differential scanning calorimetry (DSC) and saturation transfer electron paramagnetic resonance (STEPR), protein−protein interactions were detected between the bovine heart mitochondrial cytochrome *c* oxidase and F_1F_0-ATP synthase in the native membrane state (*19*), but the bovine system does not lend itself to analysis of mutations in which in vivo OXPHOS patterns are correlated with the capacity for interaction. In this study, we use these methods to study the interaction between cytochrome caa_3 and ATP synthase from alkaliphilic *B. pseudofirmus* OF4 to probe protein−protein interactions of these alkaliphile complexes. The DSC study is based on the assumption that if two lipoprotein complexes exist separately in a phospholipid vesicle, no difference in thermotropic properties will be observed between protein−phospholipid vesicles formed from a mixture of two complexes and a mixture of protein−phospholipid vesicles formed individually from each complex. Differences in the thermodenaturation temperatures and enthalpy changes would suggest a physical interaction between cytochrome caa_3 and ATP synthase. In the STEPR study, a physical interaction between cytochrome caa_3 and ATP synthase will be indicated by an increase of rotational correlation time of spin-labeled cytochrome caa_3. Herein, we report experimental details and results of DSC and STEPR studies with cytochrome caa_3 and ATP synthase embedded in phospholipid vesicles. The results of DSC and STEPR indicate that cytochrome caa_3 does interact directly with the ATP synthase in a reconstituted membrane vesicle system.

EXPERIMENTAL PROCEDURES

Materials. Spin label, 4-maleimido-2,2,6,6-tetramethyl-1-piperidine-*N*-oxyl (MSL), cytochrome *c* (horse heart, type III), and sodium cholate were purchased from Sigma. *n*-Dodecyl β-D-maltoside (DM) and *n*-octyl β-D-glucoside were from Anatrace. Asolection was obtained from Associated Concentrates, Inc., and purified according to the procedure reported by Kagama et al. (*20*). Centriprep-30 and Centricon-30 were bought from Amicon. Other chemicals were of the highest purity commercially available.

Enzyme Preparations. The F_1F_0-ATP synthase from alkaliphilic *B. pseudofirmus* OF4 was purified from everted membrane vesicles isolated from pH 10.5 grown cells essentially as reported previously (*21*), except that the ammonium sulfate fraction used for sucrose gradient centrifugation was the pellet obtained between 37% and 60% saturation (P_{37-60}). During purification, the hydrolytic activity of the preparations was assayed by the phosphate formation method of LeBel (*22*) in the presence of octyl glucoside and Na_2SO_3 (*21*). The specific activity of preparations ranged from 30 to 40 μmol of P_i released min^{-1} (mg of protein)$^{-1}$.

The four-subunit cytochrome caa_3 was purified from the resulting supernatant (S_{37-60}) by the following modifications of the original protocol (*17*). During purification, the activity of the preparations was monitored by assays of TMPD oxidase in a 20 mM Tris-HCl, pH 8.0, 1 mM EDTA, pH 8.0, buffer using 1 mM TMPD (*23*). Unless otherwise specified, all of the purification steps were carried out at 4 °C. The S_{37-60} was sequentially brought to 70% and 80% ammonium sulfate saturation, and the P_{70-80} was removed by ultracentrifugation. The S_{70-80} was diluted with 4 volumes of buffer A (10% glycerol, 10 mM NaP_i, pH 8.0, 1 mM EDTA, 0.05% dodecyl maltoside, 0.2 mM phenylmethanesulfonyl fluoride) and loaded on a hydroxyapatite column (Bio-Rad) equilibrated in the same buffer. After the column was washed with 2 bed volumes of buffer A, the column was equilibrated at room temperature and washed sequentially with 0.2 (2 bed volumes), 0.4 (3 bed volumes), and 0.6 M NaP_i, pH 8.0, in buffer A (3−4 bed volumes). The 0.6 M fraction, containing the bulk of the cytochrome caa_3, was diluted with 6 volumes of buffer B (10% glycerol, 20 mM Tris-HCl, pH 8.0, 1 mM EDTA, 0.05% dodecyl maltoside, and 0.2 mM phenylmethanesulfonyl fluoride) and

loaded on a Q-Sepharose anion-exchange column equilibrated in the same buffer. This column was washed with 5 bed volumes of buffer B and then sequentially with 0.2 M (7 bed volumes), 0.3 M (10 bed volumes), 0.4 M (7 bed volumes), and 0.5 M NaCl (4 bed volumes) in buffer B. Cytochrome caa_3 eluted principally in the 0.4 M fraction with the 0.5 M fraction containing about 30% of the eluted oxidase. The 0.4 M fraction was concentrated and used in the reconstitution experiments. The heme $a + a_3$ content of the purified oxidase preparations was >9.0 nmol (mg of protein)$^{-1}$, based on an extinction coefficient of 20.5 mM^{-1} at $A_{600-622}$ (from the mitochondrial value given in ref *24*).

Preparation of Maleimide Spin-Labeled (MSL) Cytochrome caa_3. Alkaliphilic *B. pseudofirmus* OF4 cytochrome caa_3, 20 mg/mL in 20 mM Tris-HCl, pH 8.0, containing 0.35 M NaCl, 1 mM EDTA, 0.1 mM PMSF, 0.05% dodecyl maltoside, and 10% glycerol was incubated with a 5 molar excess of MSL for 1 h at room temperature. The stock solution of MSL (10 mM) was made in 10 mM Tris-HCl/sucrose buffer, pH 8.0, containing 20% methanol. After incubation, the unreacted MSL was removed by passage through a D-salt excellulose desalting column from Pierce, equilibrated with 10 mM Tris-HCl buffer, containing 0.05% dodecyl maltoside. Fractions containing MSL-cytochrome caa_3 were pooled and concentrated by Centriprep-30 and Centricon-30 to a protein concentration of approximately 30 mg/mL. MSL-cytochrome caa_3 obtained by this method was verified to contain no free spin-label by the conventional EPR spectra.

Preparation of Cytochrome caa_3 and F_1F_0 Complex−Phospholipid Vesicles. The protein−phospholipid vesicles were prepared by the cholate dialysis method reported by Racker (*25*). The cytochrome caa_3 complex, with or without MSL labeling, alone or in combination with F_1F_0, at a protein concentration of approximately 30 mg/mL, was mixed with an asolectin micellar solution (20 mg/mL in 50 mM phosphate buffer, pH 7.4) and a sodium cholate solution [20% (w/v) in water]. The final solution contained 7 mg/mL protein, 10 mg/mL sodium cholate, and 10.5 mg/mL asolectin. After incubation at 4 °C for 60 min, the solution was dialyzed overnight against 500 volumes of 50 mM phosphate buffer, pH 7.4, with four changes of buffer to form vesicles. The protein−phospholipid vesicles formed were collected by centrifugation at 80000*g* for 1 h, and the precipitates were resuspended together in 50 mM phosphate buffer, pH 7.4, to an appropriate protein concentration depending on the assay to be used. The suspensions were used for the DSC and STEPR experiments. Although not anticipated, the vesicles prepared by the cholate dialysis procedure described above are quite uniform in size, with diameters between 20 and 40 nm (*26*). The relatively high protein to phospholipid ratio used might contribute to this uniformity. The vesicles may not be completely sealed as judged by their low oxidation control index (data not shown). This, however, does not present any complication on the work of DSC and STEPR as the essential lipid environment of the protein complex is provided.

Differential Scanning Calorimetry. All calorimetric measurements were performed with a CSC 6100 NanoII DSC from Calorimetry Science Corp. The reference and sample solutions were carefully degassed under vacuum for 15 min prior to use. A 0.50 mL sample in 50 mM K^+/Na^+ phosphate buffer, pH 7.4, was placed in the sample capillary cell, and the same amount of buffer was placed in the reference capillary cell. All DSC scans reported in this study were run at a rate of 2 °C/min. After the first scan, the samples were cooled to the original temperature and rescanned. Since after the first scan the protein was completely and irreversibly denatured, no thermotransition peaks were observed in the second scan, and the second scan could be used as a baseline. All thermodynamic analyses were carried out according to the program known as CpCal from the Nano DSC program group.

EPR Measurements. All EPR measurements were made with a Bruker EMX EPR spectrometer, using an aqueous quartz flat cell. The temperature of the microwave cavity was controlled by circulation of cooled nitrogen gas from a modified variable temperature housing assembly equipped with an electric temperature sensor. Conventional EPR spectra were recorded with instrument settings as follows: field modulation frequency, 100 kHz; modulation amplitude, 8 G; microwave frequency, 9.757 GHz; microwave power, 10.78 mW; time constant, 1310.72 ms. Saturation transfer EPR spectra were recorded using the same instrument settings as those described by Thomas et al. (*27*) and Poore et al. (*28*). A field modulation of 8 G and microwave frequency of 9.757 GHz were employed with phase-sensitive detection at 100 Hz (second harmonic) 90° out of phase. The incident microwave power was 107.80 mW. The phase was adjusted to minimize the second harmonic signal. The approximate rotational correlation time (τ_2) was obtained from the ratio of the two field lines (L″/L). The calibration curve of Thomas et al. (*27*) derived from isotropic tumbling of MSL-labeled hemoglobin was used in the calculation.

Other Analytical Methods. Protein concentration was determined by the biuret method, using bovine serum albumin as the standard (assuming 1 mg/mL has an A_{279} of 0.667). Absorption spectra were measured in a Shimadzu UV-2401 PC spectrophotometer.

RESULTS AND DISCUSSION

Thermotropic Properties of Cytochrome caa_3 and F_1F_0-Synthase Embedded in Phospholipid Vesicles. To unambiguously study the interaction between cytochrome caa_3 and F_1F_0-synthase from alkaliphilic *B. pseudofirmus* OF4, DSC studies were carried out with both complexes embedded in phospholipid (asolectin) vesicles, because these enzymes in protein−phospholipid vesicles would have an environment similar to that in membrane. The isolated complexes, singly or in combination, were embedded in phospholipid vesicles by the cholate dialysis method (*25*). A constant phospholipid to protein ratio of 1.5 was used. This ratio was chosen because our earlier intensive DSC study on the phospholipid titration of the mitochondrial cytochrome *c* oxidase complex showed that the increase in exothermic enthalpy change of thermodenaturation of the oxidase phospholipid vesicles is directly proportional to the amount of phospholipid used, up to 1 mg/mg of protein, and then becomes constant (*29*). The ratio between F_1F_0-synthase and cytochrome caa_3 varied from 0 to 1.5. If the two lipoprotein complexes have no physical interaction, then no difference in DSC characteristics should be observed between phospholipid vesicles embedded with a mixture of two complexes and a mixture of phos-

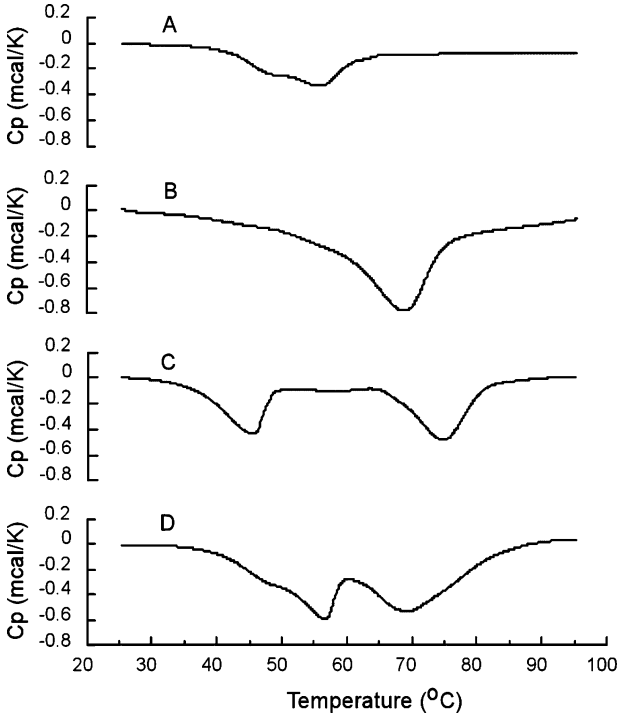

FIGURE 1: DSC curves of alkaliphilic *B. pseudofirmus* OF4 F_1F_0 and cytochrome *caa*$_3$ embedded in phospholipids singly or in combination. The molar ratio of F_1F_0 and *caa*$_3$ is 1, and the weight ratio of phospholipids to protein is 1.5 in all cases. These vesicles are prepared by the cholate dialysis method. Curve A shows the exothermic thermodenaturation of 0.5 mg of F_1F_0 embedded in phospholipid vesicles. Curve B is the DSC thermogram of 0.105 mg/mL *caa*$_3$ embedded in phospholipid vesicles. Curve C is the DSC profile of phospholipid vesicles embedded with a mixture of 0.5 mg of F_1F_0 and 0.105 mg of *caa*$_3$. Curve D is a mixture of phospholipid vesicles, embedded individually with either 0.5 mg of F_1F_0 or 0.105 mg of *caa*$_3$. A total of 21 assays were conducted on two independent preparations. The standard deviations for the transition temperatures were in the range of 0.1−0.3° and for enthalpy changes were 0.5−0.8 kcal/mmol.

pholipid vesicles embedded with one or the other complex; i.e., differences in the thermodenaturation temperatures (T_m) and enthalpy changes (ΔH) would suggest a physical interaction between these two lipoproteins. The protocol for vesicle preparation included a fixed incubation period of 60 min for the single or mixed complexes in solution before the reconsitution into vesicles. It is therefore possible that interactions between complexes during this period contribute to any overall interactions that are observed. However, any such contribution is likely to be minor since earlier assays of interactions of these two alkaliphile complexes in solution were negative (D. Hicks, unpublished data).

Figure 1 shows the differential scanning calorimetric curves of alkaliphilic *B. pseudofirmus* OF4 F_1F_0-synthase and cytochrome *caa*$_3$ embedded in phospholipids singly or in combination. When F_1F_0-synthase was embedded into phospholipid vesicles and subjected to DSC analysis, an exothermic peak at 57.2 °C with a small shoulder at 45 °C and an enthalpy change of −7.3 kcal/mmol of protein was observed (see Figure 1A). Purified cytochrome *caa*$_3$ also showed a single transition with $\Delta H = -17.8$ kcal/mmol of protein and $T_m = 68.5$ °C when it was embedded into phospholipid vesicles (Figure 1B). As expected, when F_1F_0-synthase protein−phospholipid vesicles were mixed with cytochrome *caa*$_3$ vesicles and subjected to DSC analysis

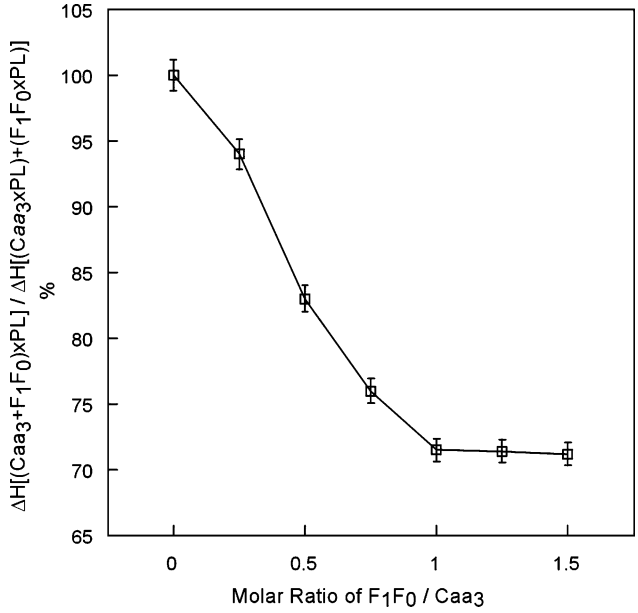

FIGURE 2: Comparison of enthalpy changes of thermodenaturation of phospholipid vesicles formed with mixtures of cytochrome *caa*$_3$ and F_1F_0-synthase from alkaliphilic *B. pseudofirmus* OF4 at various molar ratios and of mixtures of phospholipid vesicles of individual complexes. The molecular masses used in calculation of molar ratios were 517000 and 105500 Da for F_1F_0-synthase and cytochrome *caa*$_3$, respectively. The ratio of phospholipids to protein was 1.5 by weight in all cases. The data presented in error bars are averages of three assays conducted on two independent preparations.

under identical conditions, two exothermic transient peaks at 56.8 and 68.9 °C with the total ΔH of −12.4 kcal/mmol of protein were observed (see Figure 1D). The exothermic peak with a T_m of 68.9 °C is most likely due to the thermodenaturation of cytochrome *caa*$_3$ and the peak of 56.8 °C due to F_1F_0-synthase. The data from the mixed vesicles equaled the sum of the thermotropic properties of F_1F_0-synthase−phospholipid vesicles and cytochrome *caa*$_3$−phospholipid vesicles. By contrast, the protein−phospholipid vesicles formed from a mixture of F_1F_0-synthase and cytochrome *caa*$_3$ exhibited $T_{m1} = 45.5$ °C and $T_{m2} = 74.6$ °C with $\Delta H = -8.8$ kcal/mmol of protein (see Figure 1C). These data for the embedded mixture are significantly different from those observed in a mixture of phospholipid vesicles embedded individually with F_1F_0-synthase or cytochrome *caa*$_3$, suggesting that there is an interaction between these two complexes. In the vesicles prepared by embedding the mixture of complexes, the component F_1F_0-synthase and cytochrome *caa*$_3$ complexes, respectively, undergo thermodenaturation at lower and higher temperatures than in the vesicles in which a single complex is embedded alone. Since, when a mixture of F_1F_0-synthase and cytochrome *caa*$_3$ is embedded in phospholipid vesicles, the F_1F_0-synthase undergoes thermodenaturation at 45 °C (T_{m1}) (Figure 1C), the small shoulder around 45 °C in the DSC analysis of F_1F_0-synthase vesicles alone (Figure 1A) suggests that a small portion of the F_1F_0-synthase complex had characteristics similar to that present in the vesicles in which both F_1F_0-synthase and cytochrome *caa*$_3$ were incorporated. This could result from trace contamination of the F_1F_0-synthase complex preparation by an interacting subunit of cytochrome *caa*$_3$ that was not detectable in redox spectra.

Figure 2 compares the thermodenaturation enthalpy changes of phospholipid vesicles formed with mixtures of cytochrome

caa$_3$ and F_1F_0-synthase at various molar ratios and of mixtures of phospholipid vesicles of individual complexes. The value of the difference in ΔH increases as F_1F_0-synthase is increased. The maximum difference is obtained when approximately 1 mol of F_1F_0-synthase/mol of cytochrome *caa*$_3$ is used. This is consistent with the conclusion that the observed effects are due to interactions between cytochrome *caa*$_3$ and F_1F_0-synthase rather than some other interaction such as dimerization of one of the complexes or a change in lipid−protein interaction.

As discussed earlier (*19*, *26*, *29*, *30*), the energy for the exothermic transition of a protein complex embedded in phospholipid vesicles comes from the collapse, upon thermodenaturation, of a strained interaction between unsaturated fatty acyl groups of phospholipids and a protein surface on the protein complex. Little exothermic transition was observed in mitochondrial or submitochondrial preparations because there is no such exposed area in the native complex or supercomplex (*19*). When two interacting protein complexes are removed from the biological membrane by detergent solubilization, the interaction between them becomes disrupted, with the detergent masking the areas on the protein surfaces that interact. Subsequently, when protein−phospholipid vesicles are formed from the two complexes coincident with removal of the detergent, the exposed area on the protein surface becomes greatly diminished through protein−protein interaction. Therefore, less strained interaction occurs upon vesicle formation, and less enthalpy change of exothermic denaturation is observed. It has been suggested that heat release that accompanies thermodenaturation of the mitochondrial membrane under aerobic conditions may be attributable to autoxidation of iron−sulfur proteins (*31*). This suggestion is not germane to the current study because there are no iron−sulfur proteins in either cytochrome *caa*$_3$ or the F_1F_0-ATP synthase complex.

STEPR Studies of Spin-labeled Cytochrome caa$_3$ *Embedded in Phospholipid Vesicles in the Absence and Presence of F*$_1$*F*$_0$*-Synthase*. To confirm the existence of a physical interaction between alkaliphile cytochrome *caa*$_3$ and F_1F_0-synthase, cytochrome *caa*$_3$ was labeled with 4-maleimido-2,2,6,6-tetramethyl-1-piperidine-*N*-oxyl (MSL) as described under Experimental Procedures. The MSL-cytochrome *caa*$_3$, which is enzymatically active, was embedded in phospholipid vesicles alone or together with F_1F_0-synthase. The electron paramagnetic resonance (EPR) measurements of these electron transfer complex−phospholipid vesicles showed typical spin-immobilized spectra (see spectra A and B of Figure 3). The spectra were identical regardless of whether the protein−phospholipid vesicles contained only cytochrome *caa*$_3$ or cytochrome *caa*$_3$ and F_1F_0-synthase complexes (Figure 3A,B). This suggested that the difference in mobility of the spin label on cytochrome *caa*$_3$, in the absence and presence of F_1F_0-synthase, is too small to be measured by conventional EPR. Therefore, the protein rotational diffusion of the spin-labeled complex was measured by saturation transfer electron paramagnetic resonance (STEPR). From the change of the ratio of two low-field signals (L″/L) (see spectra C and D of Figure 3), rotational correlation times (τ_2) can be calculated according to reported methods (*27*, *28*). Table 1 shows the effect of the addition of F_1F_0-synthase on the rotational correlation time of spin-labeled cytochrome *caa*$_3$. When mixed with F_1F_0-synthase from alkaliphilic *B. pseudofirmus* OF4 before being embedded in phospholipid vesicles, a significant increase in τ_2 was observed compared to that of spin-labeled cytochrome *caa*$_3$ embedded in phospholipid vesicles alone. By contrast, the τ_2 of spin-labeled cytochrome *caa*$_3$ was not affected when the cytochrome *bc*$_1$ complex or ATP synthase from bovine heart mitochondria was substituted for the alkaliphile ATP synthase prior to the formation of vesicles, and the mixture of the spin-labeled cytochrome *caa*$_3$ complex and F_1F_0-synthase phospholipid vesicles showed the same τ_2 as that of cytochrome *caa*$_3$ phospholipid vesicles alone (see Table 1).

A similar effect of succinate−Q reductase on τ_2 of spin-labeled ubiquinol−cytochrome *c* reductase (*30*) and of F_1F_0-

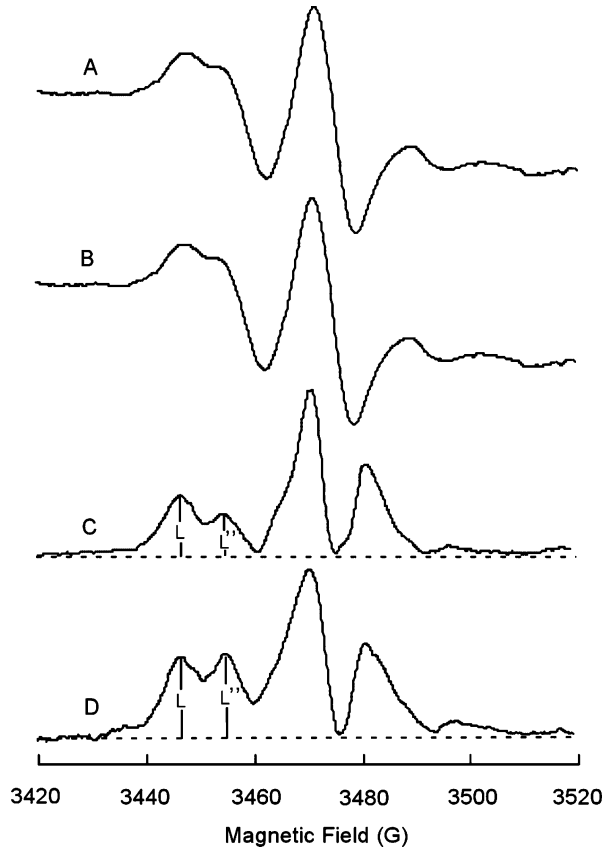

FIGURE 3: EPR spectra of spin-labeled alkaliphilic *B. pseudofirmus* OF4 cytochrome *caa*$_3$ in the presence and absence of the OF4 F_1F_0-synthase complex. Spectra A and B are conventional EPR spectra of spin-labeled OF4 cytochrome *caa*$_3$ embedded in phospholipid vesicles in the absence or presence of the OF4 F_1F_0-synthase complex. Spectra C and D are the saturation transfer EPR spectra of the same samples. The protein concentrations were 6 and 36 mg/mL for *caa*$_3$ and *caa*$_3$ + F_1F_0 vesicles, respectively. The patterns shown are typical of a total of 21 assays conducted on two independent preparations.

Table 1: Effect of Additions on the Rotational Correlation Time (τ_2) of Spin-Labeled Cytochrome *caa*$_3$[a]

preparations	L″/L	τ_2 (μs)
(MSL-*caa*$_3$)PL	0.70 ± 0.01	65 ± 2
(MSL-*caa*$_3$ + bF_1F_0)PL	1.06 ± 0.01	270 ± 1
(MSL-*caa*$_3$)PL + (bF_1F_0)PL	0.71 ± 0.01	70 ± 2
(MSL-*caa*$_3$ + mF_1F_0)PL	0.71 ± 0.01	70 ± 2
(MSL-*caa*$_3$ + m*bc*$_1$)PL	0.70 ± 0.01	65 ± 2

[a] The molar ratio of cytochrome *caa*$_3$ to other proteins used was 1:1. The data presented are averages of three assays conducted on two independent preparations.

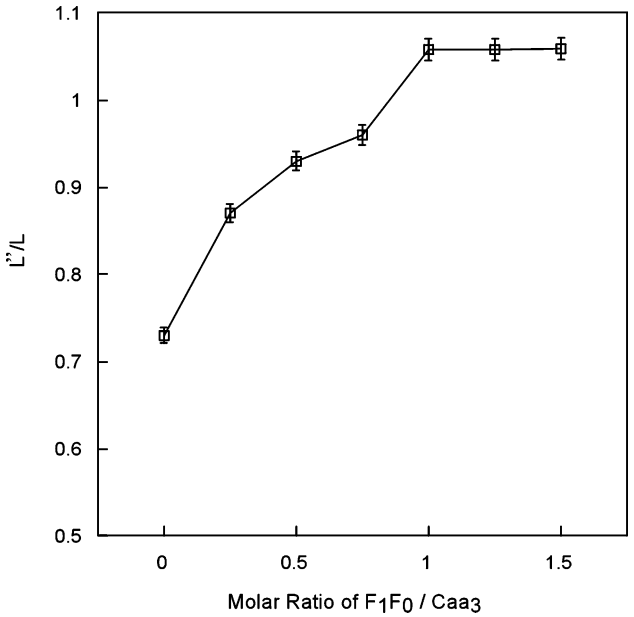

FIGURE 4: Effect of F_1F_0-synthase on STEPR of spin-labeled cytochrome *caa*$_3$. Increasing amounts of F_1F_0-synthase were added to a constant amount of spin-labeled cytochrome *caa*$_3$. The solutions were incubated for 60 min at 4 °C before being embedded in phospholipid vesicles. 1.5 mg of phospholipid/mg of protein was used in all cases. L″/L was calculated from the saturation transfer EPR spectra of each sample. Instrument settings are given under Experimental Procedures. The data shown in error bars are averages of three assays conducted on two independent preparations.

synthase on τ_2 of spin-labeled cytochrome *c* oxidase from bovine mitochondria (*19*) has been reported from this group. It is conceivable that at least part of the observed effect resulted from a change in the fluidity of the membrane by inclusion of protein complexes other than the spin-labeled complex. To ensure that the observed τ_2 increase upon mixing alkaliphile F_1F_0-synthase with spin-labeled cytochrome *caa*$_3$ is indeed due to an interaction between these two complexes, and not due to the change of protein concentration or self-aggregation upon addition of F_1F_0-synthase, a titration of spin-labeled cytochrome *caa*$_3$ with F_1F_0-synthase was carried out. If a specific interaction between these two complexes exists, it is expected that a maximum τ_2 will be obtained. As shown in Figure 4, the break point in τ_2 was obtained when the ratio of alkaliphile F_1F_0-synthase to cytochrome *caa*$_3$ approached 1, which is in consistent with the number obtained from the DSC data. We note that the rotational correlation time obtained from STEPR is only an approximate value; it is based on the calibration curve derived from the isotropic motion of the spin label. The values obtained, however, agree with those obtained by other methods, such as flash photolysis (*32*). Moreover, although our main interest in this study was the relative τ_2 of spin-labeled cytochrome *caa*$_3$ in the absence and presence of the F_1F_0-synthase from alkaliphilic *B. pseudofirmus* OF4, the τ_2 values obtained were in agreement with the DSC data (i.e., the titration curve of the τ_2 values shows the same value of 1 for the saturation as that obtained from the DSC data).

There are a growing number of reports of "supercomplexes", i.e., putative specific supermolecular structures containing more than one respiratory chain complex, in organisms ranging from bacteria (*33*−*37*), the yeast *Saccharomyces cerevisiae* (*38*, *39*), beef (*19*, *30*, *38*, *40*), and plants (*41*−*45*). Various roles have been attributed to these respiratory supercomplexes in fostering electron transfer reactions, the regulatory features of electron transport, and the membrane biological aspects of respiration (*19*, *38*, *39*, *42*, *46*, *47*). The supercomplexes are most often detected on native gel systems involving a non-native environment in which the nonionic detergents that are normally used may strongly influence the interactions. The interaction among lipoprotein complexes detected by the DSC and STEPR methods used here is less influenced by detergents used in the isolation of the complexes since the detergents are removed during the formation of vesicles. The approach was chosen because, in the vesicles, the protein complexes are in a membrane environment similar to that of the native system. This eliminates many of the possible detergent effects and, importantly, may facilitate detection of interactions that are dynamic. These approaches were chosen for the latter reason since we are not aware of data demonstrating stable complex formation between ATP synthase and the respiratory chain of bacteria or mitochondria and have never detected evidence for a "supercomplex" containing an alkaliphile respiratory chain complex and the ATP synthase during diverse purification efforts. On the basis of the results shown here, we conclude that cytochrome *caa*$_3$ and F_1F_0-ATP synthase from alkaliphilic *B. pseudofirmus* OF4 could physically interact in the membrane. These are most likely via dynamic interactions that do not form a supercomplex but make the OXPHOS model distinct from that of freely diffusible electron transfer complexes that was derived from membrane fusing (*48*) and fluorescence recovery after photobleaching (FRAP) measurements (*49*).

In the alkaliphile context, the specific interaction of the cytochrome oxidase and the ATP synthase observed here in a reconstituted system is relevant to models of the proton path during OXPHOS that posit direct protein−protein interactions. The alkaliphile system can now be used to dissect the elements involved in the interactions using mutants whose effects upon OXPHOS in vivo can also be determined. This will make it possible to test whether one or more of the alkaliphile-specific features of the ATP synthase and cytochrome *caa*$_3$ facilitate the interactions observed here and/or apparent proton sequestration in bioenergetic experiments. A candidate in the alkaliphile ATP synthase would be the unusually polar loop on the external side of the a-subunit, near the putative proton uptake pathway, that was shown to be required for optimal OXPHOS at high pH but not critically involved in the proton-gating function (*15*). A candidate of interest in the cytochrome *caa*$_3$ is the unusually acidic patch that was noted when the operon encoding the complex was first cloned and sequenced (*17*). This acidic domain is predicted to be near the region of subunit II just above where the pumped protons are modeled to emerge (*50*, *51*). Additional respiratory chain components might also be considered as possible intermediaries in proton transfer in alkaliphiles. Goto et al. (*52*) suggest that cytochrome *c* may support rapid proton translocation in conjunction with cytochrome oxidase and ATP synthase in the alkaliphile membrane.

OXPHOS in alkaliphilic *Bacillus* faces special energetic challenges at high pH because of the low Δp and the requirement for greater energy input for catalysis itself at

high pH. This has presumably provided the adaptive pressure for special features of the participating complexes to function synthetically at high pH, as so far demonstrated for the ATP synthase. In addition, alkaliphilic *Bacillus* species have higher membrane concentrations of respiratory chain complexes than most bacteria as well as unusually high membrane cardiolipin content; cardiolipin content, like key respiratory complexes, is elevated during growth at pH ≥10 than at near neutral pH (*11*, *17*). The high cardiolipin content and respiratory chain content are properties shared by alkaliphilic *Bacillus* and mitochondria. This makes it especially notable that a stoichiometric interaction between F_1F_0-ATP synthase and cytochrome *c* oxidase (an aa_3 type) of beef heart mitochondria has been observed that is comparable to the physical interaction found here for the *B. pseudofirmus* OF4 ATP synthase and cytochrome caa_3 oxidase (*17*). These observations could reflect a more general commonality in which OXPHOS in mitochondria from higher (aerobic) eukaryotes and alkaliphilic *Bacillus* are particularly subject to selection for the efficacy of energy conservation via OXPHOS. As a result, both might use a sequestered path of protons, as has been hypothesized by others (*4*−*8*). By contrast, the efficacy of OXPHOS is probably not a central limiting factor for growth of facultatively anaerobic eukaryotes, most bacteria, or even alkaliphiles at lower pH. The high cardiolipin and respiratory chain content of higher eukaryotic mitochondria and alkaliphilic *Bacillus* could be pieces of a common strategy, as could specific adaptation of these complexes, though this latter possibility cannot yet be evaluated. None of the alkaliphile-specific features of the membrane-embedded F_0-ATP synthase has yet been experimentally shown to play such a role. If such an element is identified and more structural information about the F_0-ATP synthase segments becomes available, it may become possible to assess whether a comparable adaptation exists in the alkaliphile and eukaryotic segments.

ACKNOWLEDGMENT

We thank Dr. Roger Koeppe for critical review of the manuscript.

REFERENCES

1. Mitchell, P. (1961) Coupling of phosphorylation to electron and hydrogen transfer by a chemi-osmotic type of mechanism, *Nature 191*, 144−148.
2. Boyer, P. D. (1997) The ATP synthase—a splendid molecular machine, *Annu. Rev. Biochem. 66*, 717−749.
3. Stock, D., Gibbons, C., Arechaga, I., Leslie, A. G., and Walker, J. E. (2000) The rotary mechanism of ATP synthase, *Curr. Opin. Struct. Biol. 10*, 672−679.
4. Rottenberg, H. (1985) Proton-coupled energy converstion: chemiosmotic and intramembrane coupling, *Mod. Cell Biol. 4*, 47−83.
5. Williams, R. J. P. (1961) Possible functions of chains of catalysts, *J. Theor. Biol. 1*, 1−17.
6. Williams, R. J. (1978) The multifarious couplings of energy transduction, *Biochim. Biophys. Acta 505*, 1−44.
7. Slater, E. C. (1987) The mechanism of the conservation of energy of biological oxidations, *Eur. J. Biochem. 166*, 489−504.
8. Haines, T. H., and Dencher, N. A. (2002) Cardiolipin: a proton trap for oxidative phosphorylation, *FEBS Lett. 528*, 35−39.
9. Mulkidjanian, A. Y., Cherepanov, D. A., Heberle, J., and Junge, W. (2005) Proton transfer dynamics at membrane/water interface and mechanism of biological energy conversion, *Biochemistry (Moscow) 70*, 251−256.
10. Dimroth, P., and Cook, G. M. (2004) Bacterial Na^+- or H^+-coupled ATP synthases operating at low electrochemical potential, *Adv. Microb. Physiol. 49*, 175−218.
11. Krulwich, T. A., Ito, M., Gilmour, R., Hicks, D. B., and Guffanti, A. A. (1998) Energetics of alkaliphilic *Bacillus* species: physiology and molecules, *Adv. Microb. Physiol. 40*, 401−438.
12. Krulwich, T. A., Hicks, D. B., Swartz, T. H., and Ito, M. (2006) Bioenergetic adaptations that support alkaliphily, in *Physiology and Biochemistry of Extremophiles* (Gerday, C., and Glansdorff, N., Eds.) ASM Press, Washington, DC (in press).
13. Krulwich, T. A. (1995) Alkaliphiles: "basic" molecular problems of pH tolerance and bioenergetics, *Mol. Microbiol. 15*, 403−410.
14. Guffanti, A. A., and Krulwich, T. A. (1994) Oxidative phosphorylation by ADP + P_i-loaded membrane vesicles of alkaliphilic *Bacillus firmus* OF4, *J. Biol. Chem. 269*, 21576−21582.
15. Wang, Z., Hicks, D. B., Guffanti, A. A., Baldwin, K., and Krulwich, T. A. (2004) Replacement of amino acid sequence features of a- and c-subunits of ATP synthases of alkaliphilic *Bacillus* with the *Bacillus* consensus sequence results in defective oxidative phosphorylation and non-fermentative growth at pH 10.5, *J. Biol. Chem. 279*, 26546−26554.
16. Quirk, P. G., Guffanti, A. A., Plass, R. J., Clejan, S., and Krulwich, T. A. (1991) Protonophore-resistance and cytochrome expression in mutant strains of the facultative alkaliphile *Bacillus firmus* OF4, *Biochim. Biophys. Acta 1058*, 131−140.
17. Quirk, P. G., Hicks, D. B., and Krulwich, T. A. (1993) Cloning of the *cta* operon from alkaliphilic *Bacillus firmus* OF4 and characterization of the pH-regulated cytochrome caa_3 oxidase it encodes, *J. Biol. Chem. 268*, 678−685.
18. Krulwich, T. A., Ito, M., Gilmour, R., Sturr, M. G., Guffanti, A. A., and Hicks, D. B. (1996) Energetic problems of extremely alkaliphilic aerobes, *Biochim. Biophys. Acta 1275*, 21−26.
19. Qiu, Z. H., Yu, L., and Yu, C. A. (1992) Spin-label electron paramagnetic resonance and differential scanning calorimetry studies of the interaction between mitochondrial cytochrome *c* oxidase and adenosine triphosphate synthase complex, *Biochemistry 31*, 3297−3302.
20. Kagawa, Y. (1971) Reconstitution of oxidative phosphorylation system, *Tanpakushitsu Kakusan Koso 16*, 775−786.
21. Hicks, D. B., and Krulwich, T. A. (1990) Purification and reconstitution of the F_1F_0-ATP synthase from alkaliphilic *Bacillus firmus* OF4. Evidence that the enzyme translocates H^+ but not Na^+, *J. Biol. Chem. 265*, 20547−20554.
22. LeBel, D., Poirier, G. G., and Beaudoin, A. R. (1978) A convenient method for the ATPase assay, *Anal. Biochem. 85*, 86−89.
23. Sakamoto, J., Matsumoto, A., Oobuchi, K., and Sone, N. (1996) Cytochrome bd-type quinol oxidase in a mutant of *Bacillus stearothermophilus* deficient in caa_3-type cytochrome *c* oxidase, *FEMS Microbiol. Lett. 143*, 151−158.
24. van Gelder, B. F. (1966) On cytochrome *c* oxidase. I. The extinction coefficients of cytochrome *a* and cytochrome a_3, *Biochim. Biophys. Acta 118*, 36−46.
25. Racker, E. (1972) Reconstitution of cytochrome oxidase vesicles and conferral of sensitivity to energy transfer inhibitors, *J. Membr. Biol. 10*, 221−235.
26. Gwak, S. H., Yu, L., and Yu, C. A. (1985) Studies of protein-phospholipid interaction in isolated mitochondrial ubiquinone-cytochrome *c* reductase, *Biochim. Biophys. Acta 809*, 187−198.
27. Thomas, D. D., Dalton, L. R., and Hyde, J. S. (1976) Rotational diffusion studied by passage saturation transfer electron paramagnetic resonance, *J. Chem. Phys. 65*, 3006−3024.
28. Poore, V. M., Fitzsimons, J. T., and Ragan, C. I. (1982) The effects of lipid fluidity on the rotational diffusion of complex I and complex III in reconstituted NADH-cytochrome *c* oxidoreductase, *Biochim. Biophys. Acta 693*, 113−124.
29. Yu, C. A., Gwak, S. H., and Yu, L. (1985) Studies on protein-lipid interactions in cytochrome *c* oxidase by differential scanning calorimetry, *Biochim. Biophys. Acta 812*, 656−664.
30. Gwak, S. H., Yu, L., and Yu, C. A. (1986) Spin-label electron paramagnetic resonance and differential scanning calorimetry studies of the interaction between mitochondrial succinate-ubiquinone and ubiquinol-cytochrome *c* reductases, *Biochemistry 25*, 7675−7682.
31. Knox, B. E., and Tsong, T. Y. (1984) Voltage-driven ATP synthesis by beef heart mitochondrial F_0F_1-ATPase, *J. Biol. Chem. 259*, 4757−4763.
32. Cherry, R. J. (1979) Rotational and lateral diffusion of membrane proteins, *Biochim. Biophys. Acta 559*, 289−327.

33. Berry, E. A., and Trumpower, B. L. (1985) Isolation of ubiquinol oxidase from *Paracoccus denitrificans* and resolution into cytochrome bc_1 and cytochrome *c*-aa_3 complexes, *J. Biol. Chem. 260*, 2458−2467.
34. Iwasaki, T., Matsuura, K., and Oshima, T. (1995) Resolution of the aerobic respiratory system of the thermoacidophilic archaeon, *Sulfolobus* sp. strain 7. I. The archaeal terminal oxidase supercomplex is a functional fusion of respiratory complexes III and IV with no *c*-type cytochromes, *J. Biol. Chem. 270*, 30881−30892.
35. Niebisch, A., and Bott, M. (2003) Purification of a cytochrome *bc*-aa_3 supercomplex with quinol oxidase activity from *Corynebacterium glutamicum*. Identification of a fourth subunity of cytochrome aa_3 oxidase and mutational analysis of diheme cytochrome c_1, *J. Biol. Chem. 278*, 4339−4346.
36. Sone, N., Sekimachi, M., and Kutoh, E. (1987) Identification and properties of a quinol oxidase super-complex composed of a bc_1 complex and cytochrome oxidase in the thermophilic bacterium PS3, *J. Biol. Chem. 262*, 15386−15391.
37. Stroh, A., Anderka, O., Pfeiffer, K., Yagi, T., Finel, M., Ludwig, B., and Schagger, H. (2004) Assembly of respiratory complexes I, III, and IV into NADH oxidase supercomplex stabilizes complex I in *Paracoccus denitrificans*, *J. Biol. Chem. 279*, 5000−5007.
38. Schagger, H., and Pfeiffer, K. (2000) Supercomplexes in the respiratory chains of yeast and mammalian mitochondria, *EMBO J. 19*, 1777−1783.
39. Arnold, I., Pfeiffer, K., Neupert, W., Stuart, R. A., and Schagger, H. (1998) Yeast mitochondrial F_1F_0-ATP synthase exists as a dimer: identification of three dimer-specific subunits, *EMBO J. 17*, 7170−7177.
40. Schagger, H., and Pfeiffer, K. (2001) The ratio of oxidative phosphorylation complexes I-V in bovine heart mitochondria and the composition of respiratory chain supercomplexes, *J. Biol. Chem. 276*, 37861−37867.
41. Ferguson-Miller, S., Hochman, J., and Schindler, M. (1986) Aggregation and diffusion in the mitochondrial electron transfer chain: role in electron flow and energy transfer, *Biochem. Soc. Trans. 14*, 822−824.
42. Eubel, H., Jansch, L., and Braun, H. P. (2003) New insights into the respiratory chain of plant mitochondria. Supercomplexes and a unique composition of complex II, *Plant Physiol. 133*, 274−286.
43. Eubel, H., Heinemeyer, J., and Braun, H. P. (2004) Identification and characterization of respirasomes in potato mitochondria, *Plant Physiol. 134*, 1450−1459.
44. Dudkina, N. V., Eubel, H., Keegstra, W., Boekema, E. J., and Braun, H. P. (2005) Structure of a mitochondrial supercomplex formed by respiratory-chain complexes I and III, *Proc. Natl. Acad. Sci. U.S.A. 102*, 3225−3229.
45. Krause, F., Reifschneider, N. H., Vocke, D., Seelert, H., Rexroth, S., and Dencher, N. A. (2004) "Respirasome"-like supercomplexes in green leaf mitochondria of spinach, *J. Biol. Chem. 279*, 48369−48375.
46. Acin-Perez, R., Bayona-Bafaluy, M. P., Fernandez-Silva, P., Moreno-Loshuertos, R., Perez-Martos, A., Bruno, C., Moraes, C. T., and Enriquez, J. A. (2004) Respiratory complex III is required to maintain complex I in mammalian mitochondria, *Mol. Cell 13*, 805−815.
47. Paumard, P., Vaillier, J., Coulary, B., Schaeffer, J., Soubannier, V., Mueller, D. M., Brethes, D., di Rago, J. P., and Velours, J. (2002) The ATP synthase is involved in generating mitochondrial cristae morphology, *EMBO J. 21*, 221−230.
48. Schneider, H., Lemasters, J. J., Hochli, M., and Hackenbrock, C. R. (1980) Liposome-mitochondrial inner membrane fusion. Lateral diffusion of integral electron transfer components, *J. Biol. Chem. 255*, 3748−3756.
49. Gupte, S., Wu, E. S., Hoechli, L., Hoechli, M., Jacobson, K., Sowers, A. E., and Hackenbrock, C. R. (1984) Relationship between lateral diffusion, collision frequency, and electron transfer of mitochondrial inner membrane oxidation-reduction components, *Proc. Natl. Acad. Sci. U.S.A. 81*, 2606−2610.
50. Hosler, J. P., Ferguson-Miller, S., and Mills, D. A. (2006) Energy transduction: proton transfer through the respiratory complexes, *Annu. Rev. Biochem. 75*, 165−187.
51. Megehee, J. A., Hosler, J. P., and Lundrigan, M. D. (2006) Evidence for a cytochrome *bcc*−aa_3 interaction in the respiratory chain of *Mycobacterium smegmatis*, *Microbiology 152*, 823−829.
52. Goto, T., Matsuno, T., Hishinuma-Narisawa, M., Yamazaki, K., Matsuyama, H., Inoue, N., and Yumoto, I. (2005) Cytochrome *c* and bioenergetic hypothetical model for alkaliphilic *Bacillus* spp., *J. Biosci. Bioeng. 100*, 365−379.

BI0619167